Journal of Inflammation Research Dovepress

Open Access Full Text Article ORIGINAL RESEARCH

# Study on the Mechanism of UMI-77 in the Treatment of Sepsis-Induced Acute Lung Injury Based on Transcriptomics and Metabolomics

Jiatian Zhang[1,*], Zhelin Xia[2,*], Cuicui Dong[3], Jiaqi Zhu[3], Hang Ni[1], Yubin Xu[2,*], Yinghe Xu[4,*]

[1]Department of Critical Care Medicine, Taizhou Hospital of Zhejiang Province, Shaoxing University, Shaoxing, 312000, People's Republic of China; [2]Department of Pharmacy, Taizhou Central Hospital (Taizhou University Hospital), Taizhou, 318000, People's Republic of China; [3]Taizhou Hospital of Zhejiang Province Affiliated to Wenzhou Medical University, Taizhou, 317000, People's Republic of China; [4]Department of Critical Care Medicine, Taizhou Hospital of Zhejiang Province Affiliated to Wenzhou Medical University, Taizhou, 317000, People's Republic of China

*These authors contributed equally to this work

Correspondence: Yubin Xu, Department of Pharmacy, Taizhou Central Hospital (Taizhou University Hospital), Taizhou, 318000, People's Republic of China, Email xuyubin1988@126.com; Yinghe Xu, Department of Critical Care Medicine, Taizhou Hospital of Zhejiang Province Affiliated to Wenzhou Medical University, Taizhou, 317000, People's Republic of China, Email xuyh@tzc.edu.cn



**Introduction:** Sepsis-induced acute lung injury (ALI), a critical sequela of systemic inflammation, often progresses to acute respiratory distress syndrome, conferring high mortality. Although UMI-77 has demonstrated efficacy in mitigating lung injury in sepsis, the molecular mechanisms underlying its action have not yet been fully elucidated.

**Methods:** This study aimed to delineate the mechanism by which UMI-77 counteracts sepsis-induced ALI using comprehensive transcriptomic and metabolomic analyses.

**Results:** UMI-77 significantly ameliorated histopathological changes in the lungs of mice with sepsis-induced ALI Transcriptomic analysis revealed that 124 differentially expressed genes were modulated by UMI-77 and were predominantly implicated in chemokine-mediated signaling pathways, apoptosis regulation, and inflammatory responses. Integrated metabolomic analysis identified Atp4a, Ido1, Ctla4, and Cxcl10 as key genes, and inosine 5'-monophosphate (IMP), thiamine monophosphate, thymidine 3',5'-cyclic monophosphate (dTMP) as key differential metabolites. UMI-77 may regulate key genes (Atp4a, Ido1, Ctla4, and Cxcl10) to affect key metabolites (IMP, thiamine monophosphate, and dTMP) and their target genes (Entpd2, Entpd1, Nt5e, and Hprt) involved in cytokine-cytokine receptor interaction, gastric acid secretion, pyrimidine, and purine metabolism in the treatment of sepsis-induced ALI.

**Conclusion:** UMI-77 exerts its therapeutic effect in sepsis-induced ALI through intricate modulation of pivotal genes and metabolites, thereby influencing critical biological pathways. This study lays the groundwork for further development and clinical translation of UMI-77 as a potential therapeutic agent for sepsis-associated lung injuries.

**Keywords:** sepsis-induced ALI, inflammation, genes, metabolites, cytokine signaling

## Introduction

Sepsis-induced acute lung injury (ALI), a critical complication of sepsis, is characterized by an excessive inflammatory response that can lead to acute respiratory distress syndrome (ARDS) and potentially fatal respiratory failure.[1] The pathophysiology of sepsis-induced ALI involves the activation of immune cells and the release of a cascade of pro-inflammatory cytokines and chemokines, which cause endothelial and epithelial damage, increased vascular permeability, and subsequent pulmonary edema.[2,3] The clinical manifestations of sepsis-induced ALI include hypoxemia, tachypnea, and bilateral infiltrates on chest imaging, which is consistent with the diagnosis of ARDS.[4,5] Septic patients with ALI also exhibit higher mortality rates and poorer prognoses, despite progress in machine support ventilation and symptomatic treatment.[6] To reduce sepsis-related mortality, it is extremely important to relieve ALI caused by sepsis.

Received: 9 October 2024
Accepted: 15 December 2024
Published: 18 December 2024

UMI-77 is a known drug candidate for pancreatic cancer,[7] glioma[8] and Alzheimer's disease.[9] A previous study found that 7.0 mg/kg UMI-77 significantly improved the 5-day survival rate of septic mice by inhibiting the inflammatory storm, and pathological results showed that UMI-77 could significantly improve the inflammatory infiltration of the lung tissue in septic mice,[10] but the mechanism of UMI-77 anti-septic-induced ALI has not been thoroughly studied. This study aimed to analyze the mechanism of action of UMI-77 against septic ALI based on transcriptomic and metabolomic data, which would lay the foundation for the development of new drugs and clinical studies of UMI-77.

# Materials and Methods

## Animal Experiments and Sample Collection

Male BALB/c mice with a specific pathogen-free (SPF) status (weight 18–22 g) were obtained from Zhejiang Weitong Lihua Experimental Animal Technology Co., Ltd. (Zhejiang, China; laboratory animal license, SYXK (Zhe): 2021–0013). All animal experiments were approved by the Taizhou University Animal Ethics Committee (ID number TZXY-2022-20221015) according to National Institute of Health's guidelines with regard to the principles of animal care (2011) and were conducted under SPF laboratory conditions.

Based on our previous study, BALB/c mice were randomly divided into three groups (control, LPS, and UMI-77 groups, n=8, respectively). Mice in the LPS and UMI-77 groups were intravenously injected with 18 mg/kg LPS (Sigma, Shanghai, China), whereas mice in the control group were administered an equal volume of saline. Mice in the UMI-77 group received daily intraperitoneal injections of 7.0 mg/kg UMI-77 (Sigma, Shanghai, China), whereas the control and model groups received an equal volume of matrix solution for five days. After the last administration, the mice were sacrificed, lung tissues were obtained and stored at −80°C and part of them were immersed in 4% paraformaldehyde.

## H&E Staining

Lung tissues from each group (n=8) were embedded in paraffin, sliced, and stained with hematoxylin and eosin (H&E) as described in a previous study. Sections were visualized under a light microscope (CX33; OLYMPUS Corporation, Tokyo, Japan).

## Transcriptomics Study

RNA from lung tissue samples was isolated and purified using TRIzol reagent (Thermo Fisher, 15596018) according to the manufacturer's protocol. The total RNA concentration and purity were determined, and concentrations > 50ng/L, RIN value> 7.0, and total RNA > 1 μg were used in further studies. Then the PolyA mRNAs were captured, after fragmentation, first strand synthesis, second strand synthesis with dUTP, end repair, 3' Adenylation, adapt ligation and UDG treatment of these procedures, they were finally sequenced using illumina NovaseqTM 6000 in standard operation, and the sequencing mode was PE150 according to the reference.[11]

After obtaining the sequencing data, the sequencing data were filtered to obtain high-quality sequencing data (Clean Data), which were then compared to the reference genome of the project species, and gene expression was quantified.

## Untargeted Metabolomics Study

Take 25mg of the lung tissues from each group (n=8) in the EP tube with homogenate beads, and 500 μL of extract (methanol: acetonitrile: water =2:2:1 (V/V)) contains the isotope-labeled internal standard was added, vortex mixed evenly for 30s and homogenate at 35Hz for 4min, then transferred to the ice water bath for 5min, this step is repeated 3 times; after stand at −40°C for 1 h, the sample was centrifuged at 4°C, 12000 rpm for 15 min to obtain the supernatant for machine testing. All samples were mixed with an equal amount of supernatant from the QC samples for machine detection. Vanquish (Thermo Fisher Scientific) ultra-performance liquid chromatography was used separated the target compounds, for polar metabolites, the Waters ACQUITY UPLC BEH Amide (2.1 mm × 100 mm, 1.7 μm) liquid chromatography column was used, and the mobile phase containing 25 mmol/L ammonium acetate and 25 mmol/L ammonia hydroxide in aqueous (A) and acetonitrile (B); for nonpolar metabolites, the Phenomenex Kinetex C18 (2.1 mm × 100 mm, 2.6 μm) liquid chromatography column was used, and the mobile phase containing 0.01% acetic acid in

aqueous and isopropyl alcohol: acetonitrile (1:1, v/v) (B). The injection volume was 2μL, the remaining conditions were in agreement with literature.[12]

MS/MS spectra were acquired using an Orbitrap Exploris 120 mass spectrometer in information-dependent acquisition mode (IDA) using Thermo Xcalibur acquisition software. The ESI source conditions were set as following: 50Arb for the sheath gas and 15Arb for the aux gas, an ESI temperature of 320 °C, 60000 for the full MS resolution, 15000 for the MS/MS resolution, SNCE 20/30/40 for collision energy, and 3.8 kV (positive) or −3.4 kV (negative) for the spray voltage, respectively.

ProteoWizard was used to convert the raw data to the mzXML format, and peak detection, extraction, alignment, and integration were performed using R based on XCMS. Metabolites were identified using the R package and BiotreeDB (V3.0).

## Bioinformatics Analysis

Transcriptomic and metabolomic analyses revealed genes and metabolites with significant differential expression that were further analyzed using bioinformatic tools. Principal component analysis (PCA) and orthogonal partial least-squares discriminant analysis (OPLS-DA) were performed using SIMCA 14.1 software (Umetrics). Gene Ontology (GO) annotation and pathway enrichment were identified using the GO database (http://www.geneontology.org) and KEGG database (https://www.kegg.jp/kegg), respectively.

## Molecular Docking

Molecular docking was performed as previously study.[10] The 3D coordinates of Atp4a (PDB ID: 8IJV), Ido1 (PDB ID: 8ABX), Ctla4 (PDB ID: 8DS7), Cxcl10 (PDB ID: 8K2X), Entpd2 (PDB ID: 3CJ1), Nt5e (PDB ID: 4H2B), and Hprt (PDB ID: 6D9S) were downloaded from the PDB database (http://www.rcsb.org/pdb/home/home.do), while those of Entpd1 (AlphaFoldDB ID: AF-P49961-F1) were downloaded from the UniProt database (https://www.uniprot.org).

## ELISA Assay

To further confirm these results, the key genes were validated by ELISA according to K-X Biotechnology (Shanghai, China) instructions.

## Statistical Analysis

SPSS 20.0 (Chicago, Armonk, NY, USA) was used for statistical analysis. Dunnett's test under one-way analysis of variance (ANOVA) was used to determine the significance of differences among the groups in transcriptomics and metabolomics study, whereas the *t*-test was used to compare the two groups. All values are expressed as mean ± standard deviation. $P < 0.05$ was set as the significant threshold.

# Results

## The Effect of UMI-77 on Lung Pathology in Septic Mice

Histological examination was performed to evaluate the effect of UMI-77 on the lung tissues of septic mice. The lung tissue in mice from the LPS group exhibited thicker and more fragmented alveolar cavities than that in the control group, with a notable presence of inflammatory cell infiltration. In contrast, treatment with UMI-77 significantly ameliorated the pathological changes in the lungs. (Figure 1).

## Lung Transcriptomics Characteristics of Septic Mice Treated by UMI-77

DESeq2 software was used to analyze the differential gene expression between the two groups. Genes were deemed differentially expressed if they had a false discovery rate (FDR) below 0.05 and an absolute fold change of at least 2 (Figure 2a and b). A total of 124 differentially expressed genes were identified among the three groups; 45 genes exhibited increased expression in the LPS group and decreased expression in the UMI-77 group, whereas 79 genes showed the opposite pattern, with decreased expression in the LPS group and increased expression in the UMI-77 group.

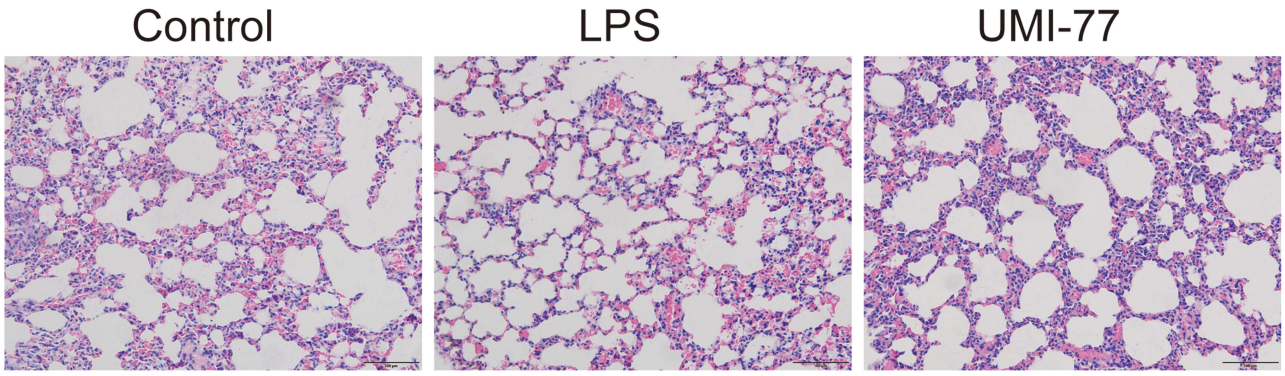


**Figure 1** The histomorphological changes of lung tissue in mice. Magnification of ×400, scale bar = 100 μm.

(Figure 2c and d; Tables S1 and S2, respectively). The gene ontology (GO) terms of the differentially expressed genes were analyzed (Figure 2e–g). Notably, the biological process GO terms for chemokine-mediated signaling pathways, positive regulation of the apoptotic process, and inflammatory response stood out. Additionally, cellular component GO terms indicated high enrichment of differentially expressed genes related to the extracellular region and space. In terms of molecular function, GO terms for CXCR/CXCR3 chemokine receptor binding and protein binding were significantly represented among the differentially expressed genes. These findings suggest a substantial impact on the regulation of immune response and cell death mechanisms.

## Metabolomics Analysis of Lung Tissue from Septic Mice Treated by UMI-77

The differential metabolites were identified with a VIP score exceeding 1 and a p-value less than 0.05, to distinguish the two groups by OPLS-DA analysis. The OPLS-DA score and permutation plots are shown in Figure 3a–d, which suggest that the model has a reliable foundation for metabolite profiling and group discrimination.[13] A total of 382 differential metabolites were identified among the three groups, 225 of which were upregulated and 157 downregulated in the LPS group compared to the control group. UMI-77 demonstrated the ability to concurrently counteract the effects of these metabolites (Figure 3e and f, Table S3).

## Integrated Analysis of Lung Transcriptomics and Metabolomics

To assess the comprehensive therapeutic impact of UMI-77 on septic-induced ALI, Spearman correlation analysis was employed to further explore the associations between the 124 differential genes and 382 differential metabolites. A total of 203 correlations between the genes and metabolites were observed, meeting the criteria of $p < 0.05$, $r > 0.7$ or $r < -0.7$ (Table S4). As demonstrated in Figure 4, 42 genes (Hoxb9, Il24, Ankk1, Ctla4, Gm37660, Trim30d, Hopxos, Gm8292, Gm13864, Lor, Chga, Gm13904, Gm7613, Gm8662, Gm8318, Majin, Gm48868, Gm45053, Ido1, Ubd, Mx1, Cxcl9, Ifit2, Gm3671, Gm5599, Gm10268, Gm7695, Gm8724, Gm15441, Gm14046, Rps12-ps19, Gm13665, Gm15289, Gm14048, Cxcl10, Cxcl11, Atp4b, Atp4a, Clps, Ghrl, Sst and Pgc) and 15 metabolites (Dodecanedioic acid, 1-Linoleoylglycerol, 2-(1-Hydroxycyclohexyl)butanoic acid, Decatrienoylcarnitine, DG 34:4, Inosine 5'-monophosphate (IMP), PG 18:0_22:6, PG 20:4_22:6, PG 22:6_22:6, Phe-Gly-Gly, SHexCer 38:5;3O, SL 10:0;O/10:0, Thiamine monophosphate, Thymidine 3',5'-cyclic monophosphate and Tridecanedioic acid) were selected for pathway analysis. As shown in Figure 5a, joint pathway analysis indicated that these integrated pathways, such as viral protein interaction with cytokine and cytokine receptors, gastric acid secretion, toll-like receptor signaling pathway, cytokine-cytokine receptor interaction, chemokine signaling pathway, growth hormone synthesis, secretion and action, thiamine metabolism, pyrimidine metabolism, and purine metabolism, are involved in the mechanism of UMI-77 in the treatment of sepsis-induced ALI.

To further clarify the relationship between differential genes and metabolites, the related targets of the metabolites were explored. The differential metabolites were analyzed using the MetScape plugin in Cytoscape to construct a metabolite-gene network, which yielded a total of 37 metabolite targets (Figure 5b). Subsequently, a protein-protein

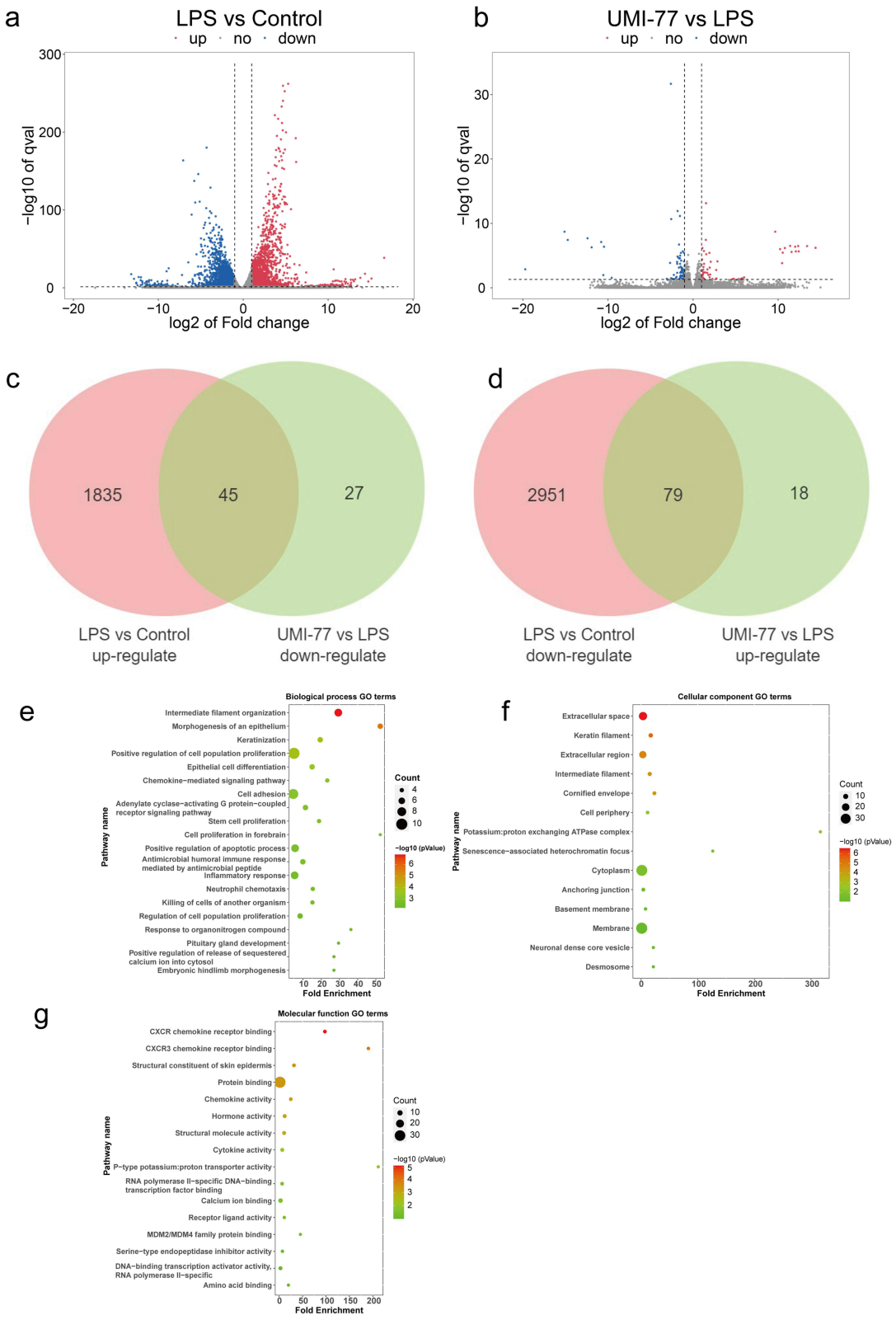


**Figure 2** Transcriptomics landscape of lung tissue from septic mice treated by UMI-77. (**a**) Volcano plot of differentially expressed genes (LPS group vs Control group), red: up-regulated, blue: down-regulated. (**b**) Volcano plot of differentially expressed genes (UMI-77 group vs LPS group), red: up-regulated, blue: down-regulated. (**c** and **d**) Venn diagram of differentially expressed genes among three groups. (**e**) Biological process GO terms. (**f**) Cellular component GO terms. (**g**) Molecular function GO terms.

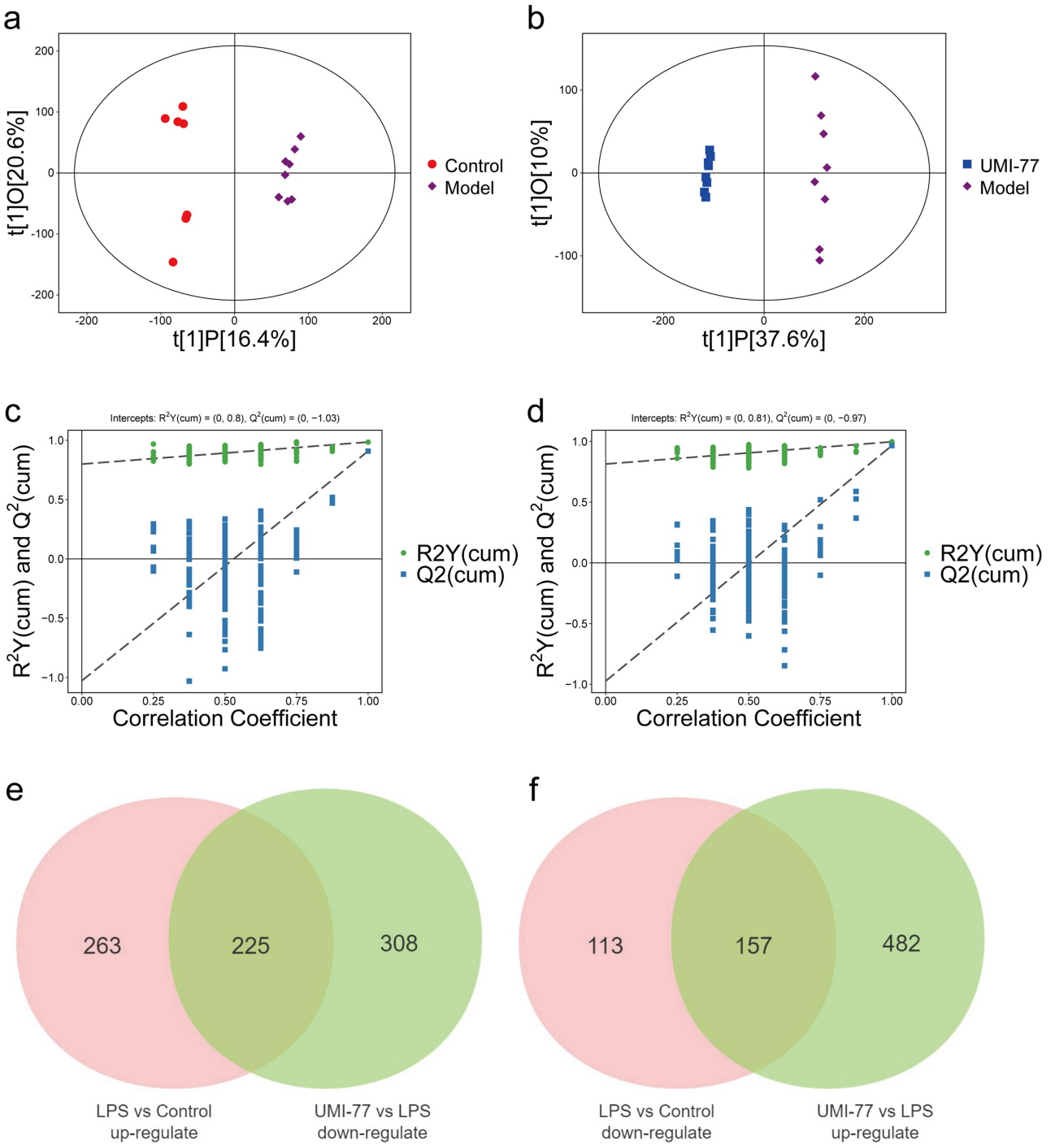


**Figure 3** Metabolomics landscape of lung tissue from septic mice treated by UMI-77. (**a**) OPLS-DA analysis (LPS group vs Control group). (**b**) OPLS-DA analysis (UMI-77 group vs LPS group). (**c**) Permutation test (LPS group vs Control group). (**d**) Permutation test (UMI-77 group vs LPS group). (**e** and **f**) Venn diagram of differentially metabolites among three groups.

interaction (PPI) network of 37 metabolite targets and 42 genes was constructed using the STRING database (https://string-db.org/), resulting in four key targets: Atp4a, Ido1, Ctla4, and Cxcl10, which are directly associated with the targets (Entpd2, Entpd1, Nt5e, and Hprt) of thymidine 3',5'-cyclic monophosphate (dTMP), inosine 5'-monophosphate (IMP), and thiamine monophosphate (Figure 5c and d). These key targets and metabolites are involved in cytokine-cytokine receptor interactions, gastric acid secretion, pyrimidine metabolism, and purine metabolism.

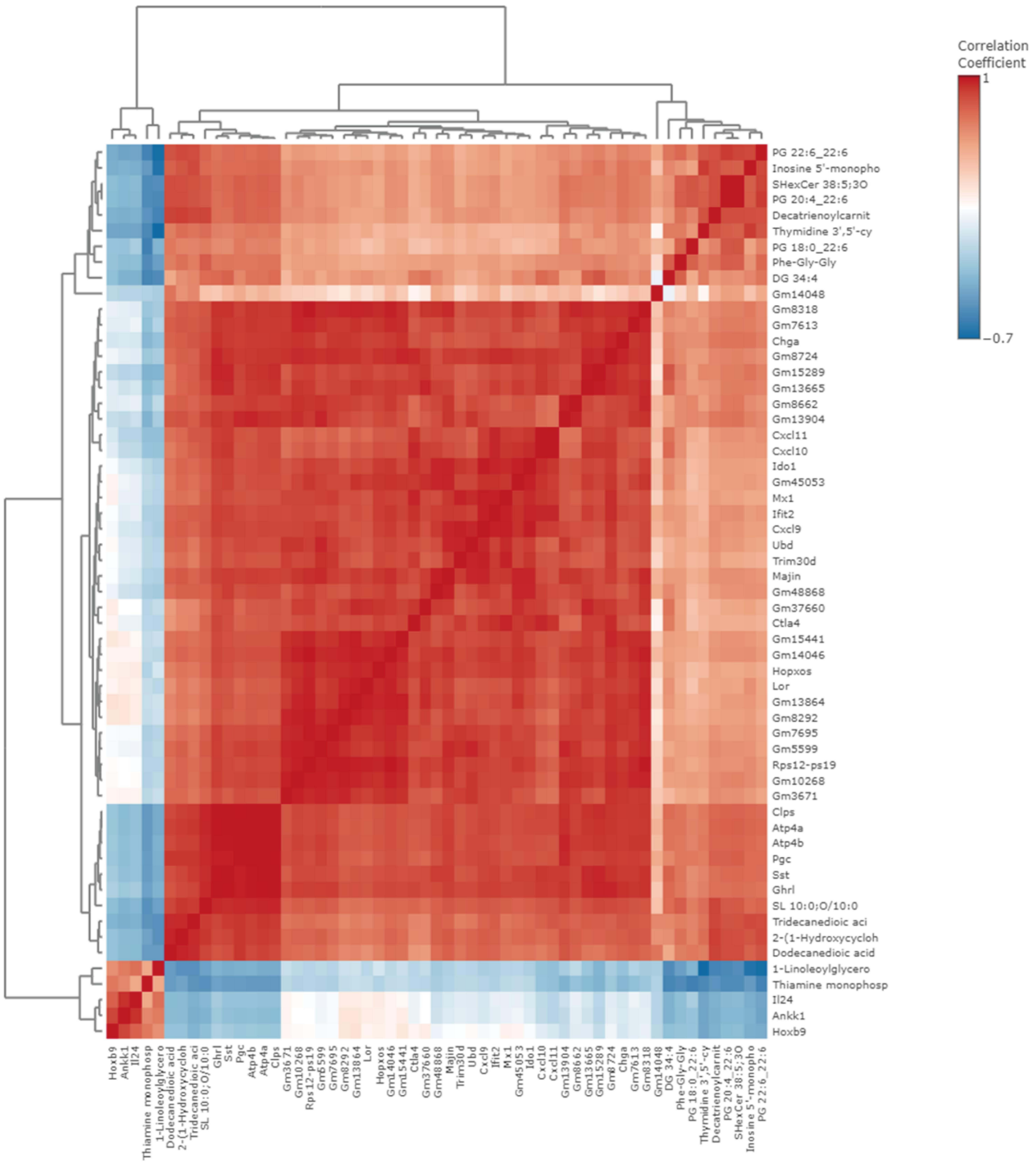


**Figure 4** The correlation heatmaps of 42 genes and 15 metabolites.

## Validation of Key Genes from Sepsis Induced ALI Mice Treated by UMI-77

ELISA and molecular docking analyses were performed to validate these results. The results showed that the levels of Atp4a, Ido1, Ctla4, Cxcl10, Entpd2, Entpd1, Nt5e, and Hprt were upregulated in the LPS group compared with those in the control group, whereas they were downregulated in the UMI-77 group (Figure 6). Results showed that UMI-77 bound to Entpd2, Nt5e, Hprt, Ido1, Ctla4, Atp4a, Cxcl10 and Entpd1 through visible hydrogen bonds, and the binding energy was −8.6 kcal/mol, −9.8 kcal/mol, −8.4 kcal/mol, −9.4 kcal/mol, −6.8 kcal/mol, −6.8 kcal/mol, −6.9 kcal/mol, −7.9 kcal/

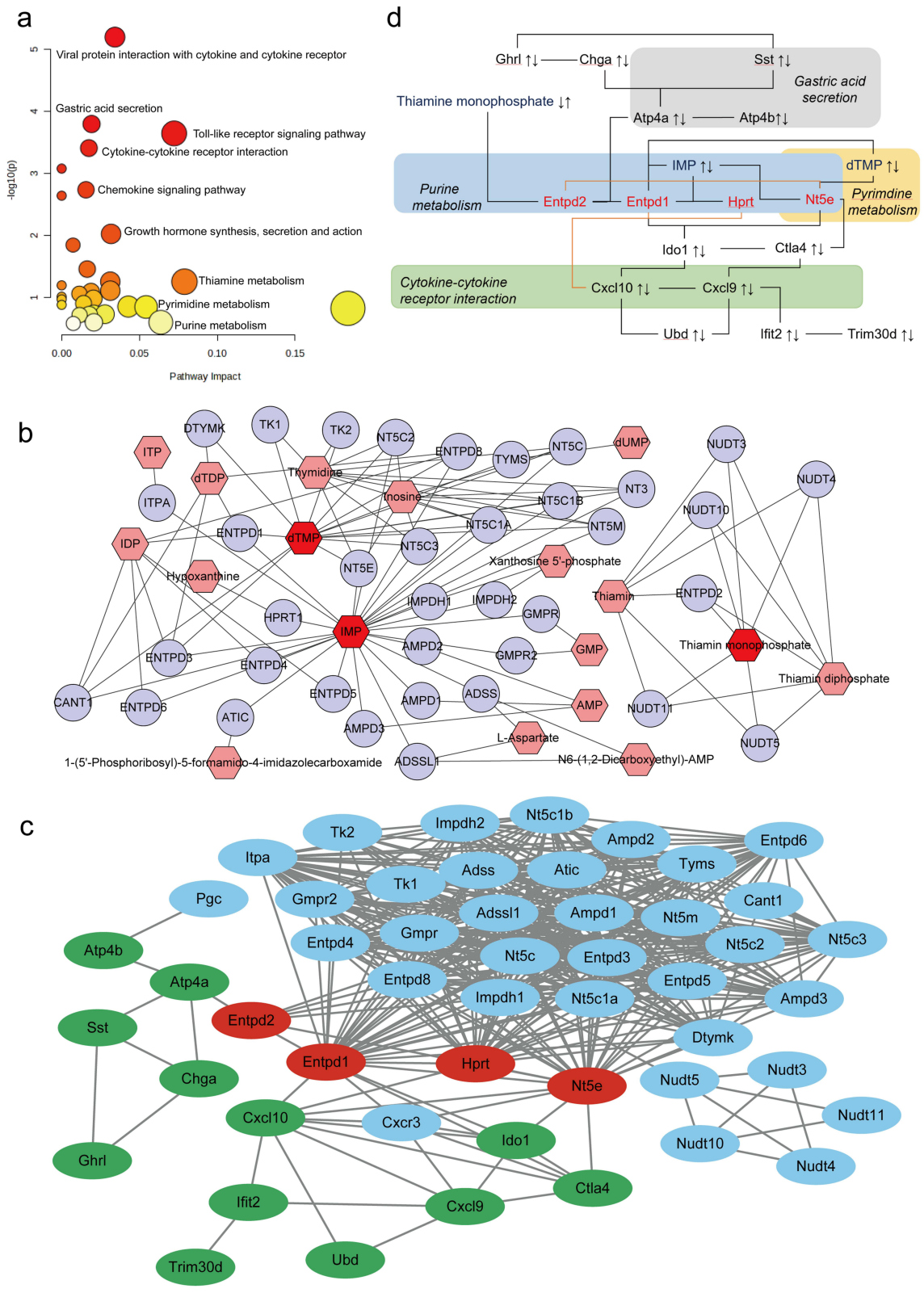


**Figure 5** Integrated analysis of lung transcriptomics and metabolomics. (**a**) The integrated pathway analysis of 42 genes and 15 metabolites. (**b**) The metabolites–genes network constructed by MetScape. (**c**) PPI network of genes and metabolites targets. (**d**) Network of genes, metabolites and metabolites targets. "↑" represented up-regulated, while "↓" represented down-regulated, the left mean LPS vs Control and the right mean UMI-77 vs LPS.

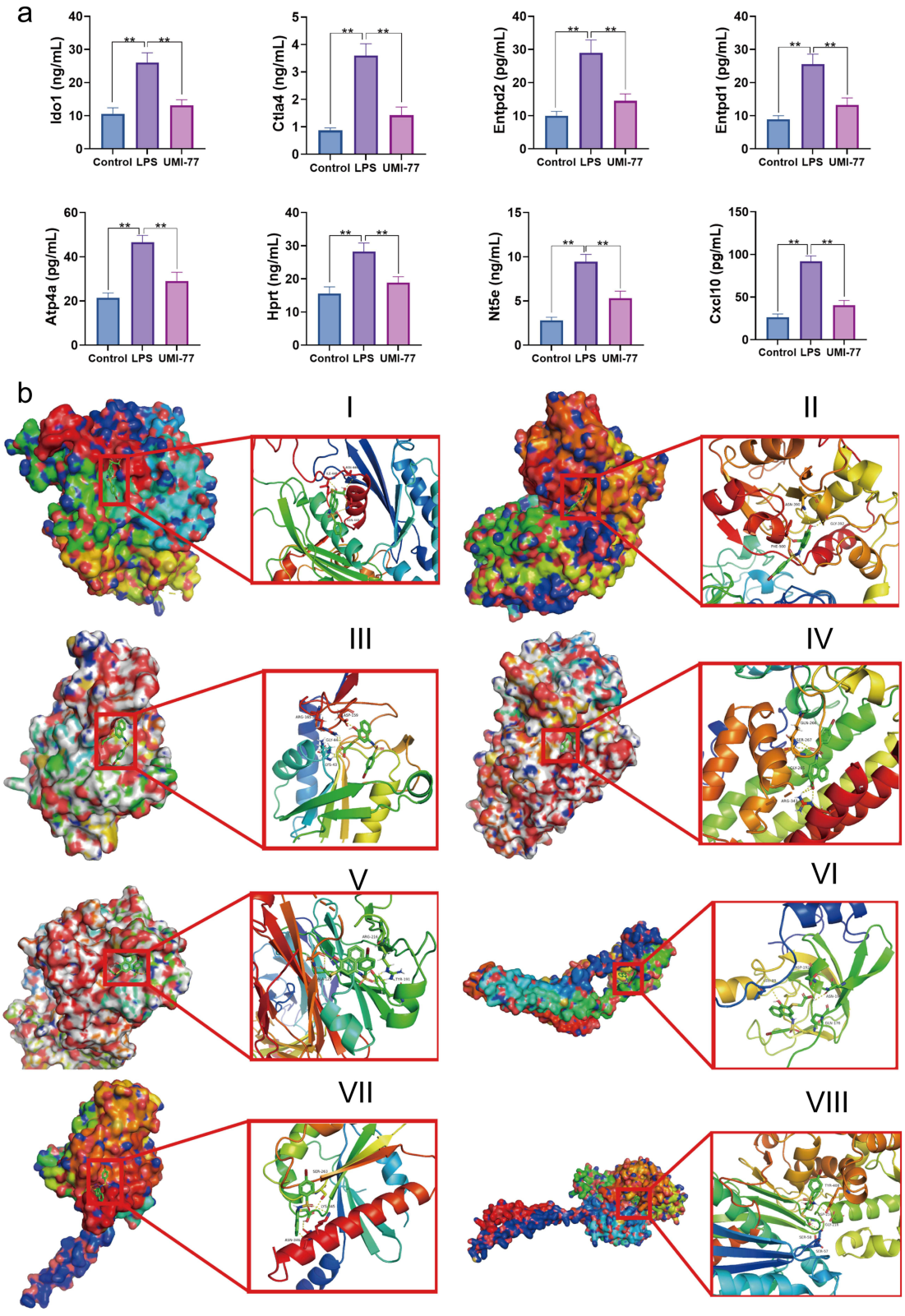


**Figure 6** Validation of key genes. (**a**) ELISA-based validation of key genes. **p<0.01. (**b**) Binding mode of UMI-77 to key genes by molecular docking. (I) Binding mode of UMI-77 to Entpd2. (II) Binding mode of UMI-77 to Nt5e. (III) Binding mode of UMI-77 to Hprt. (IV) Binding mode of UMI-77 to Ido1. (V) Binding mode of UMI-77 to Ctla4. (VI) Binding mode of UMI-77 to Atp4a. (VII) Binding mode of UMI-77 to Cxcl10. (VIII) Binding mode of UMI-77 to Entpd1.

mol, respectively, which suggesting stable binding interaction. These findings validated the significance of these pivotal genes in the therapeutic mechanism of UMI-77 in sepsis-induced ALI.

## Discussion

There are no specific drugs available for sepsis-induced ALI. In our study, we found the lung architecture of mice subjected to LPS challenge, characterized by thickened and fragmented alveolar walls and pronounced inflammatory cell infiltration, which are consistent with the hallmark features of acute respiratory distress syndrome; while 7.0 mg/kg UMI-77 can remarkable ameliorative effect on the lung's pathological state of the model mice. Thus, transcriptomics and metabolomics were used to elucidate the mechanism of action of UMI-77 in sepsis-induced ALI.

In the transcriptomics study, 124 differential genes were identified and enriched in chemokine-mediated signaling pathways, positive regulation of the apoptotic process, and inflammatory response for the biological process GO terms. Chemokine-mediated signaling pathways represent a complex network of interactions that contribute to the recruitment of immune cells, vascular changes, and tissue damage in the lungs, which are integral to the inflammatory processes that drive sepsis-induced ALI.[14,15] The apoptotic process plays a vital role in the pathogenesis and progression of sepsis-induced ALI,[16,17] and UMI-77 as an autophagy inducer, may influence the positive regulation of apoptosis by modulating the expression of genes and proteins involved in the apoptotic pathway.[8] In summary, the interplay between autophagy, apoptosis, and inflammation is central to the cellular response to sepsis, and UMI-77's ability to modulate these pathways may have significant implications for the treatment of sepsis-induced ALI.

In addition, 382 differential metabolites were identified by metabolomics and 15 metabolites closely related to the differential genes were selected for further analysis. Among these, Glycerophospholipids such as PG 18:0_22:6, PG 20:4_22:6, and PG 22:6_22:6 were upregulated, whereas DG 34:4 was downregulated in the LPS group. Sepsis-induced ALI is characterized by increased permeability of the alveolar-capillary barrier. In this context, glycerophospholipids play a crucial role in preserving the cell membrane structure, which helps regulate alveolar pressure, averting the accumulation of alveolar edema, and thereby safeguarding against alveolar collapse.[18] Fatty acids, including dodecanedioic acid, decatrienoylcarnitine, tridecanedioic acid, and 1-linoleoylglycerol, have potent effects on inflammation, vascular tone, and the immune response, all of which are critical in the pathogenesis of sepsis-induced ALI.[19–21]

Interestingly, inosine 5'-monophosphate (IMP), thiamine monophosphate, thymidine 3',5'-cyclic monophosphate (dTMP), and their targets (Entpd2, Entpd1, Nt5e, and Hprt), which are directly associated with key differential genes (Atp4a, Ido1, Ctla4, and Cxcl10), are involved in purine and pyrimidine metabolism. IMP is a nucleotide that serves as an intermediate in the purine metabolism pathway.[22] During sepsis, the metabolic demands of cells increase significantly, disrupting the balance of purine metabolism.[23] IMP, as part of this metabolic pathway, can reflect cellular stress and energy status in sepsis-induced ALI. Thiamine monophosphate, an active form of thiamine (vitamin B1) critical for energy metabolism, can be depleted due to heightened oxidative stress in sepsis, which potentially leads to thiamine deficiency that impairs energy metabolism and may exacerbate lung injury.[24] dTMP is a central molecule in pyrimidine metabolism, and is essential for DNA replication and cell proliferation.[25] The proliferation of alveolar epithelial and immune cells may be accelerated in response to injury and inflammation during sepsis, and dTMP is required for cell proliferation.[26] Moreover, their targets, including Entpd2, Entpd1, Nt5e, and Hprt, may play important roles in sepsis-induced ALI. Hprt facilitates the conversion of hypoxanthine into IMP, which serves as a precursor for AMP synthesis,[27] while Nt5e catalyzes the transformation of AMP into adenosine, a molecule that modulates vascular tone and immune reactions.[28] Entpd2 and Entpd1 hydrolyze nucleotide triphosphates to diphosphates and play a role in the regulation of extracellular nucleotide levels, which can influence purinergic signaling and immune responses.[29,30] Specifically, the modulation of Entpd2, Entpd1, Hprt, and Nt5e by UMI-77 could influence the production of extracellular adenosine, which is implicated in immune responses and inflammation, and is a key factor in the pathogenesis of sepsis-induced ALI.

In addition, in sepsis, high expression of Ido1 depletes tryptophan, accumulates canine urine, induces apoptosis and dysfunction of effector T cells, activates regulatory T cells (Tregs), and creates a microenvironment of immunosuppression.[31] Elevated levels of Ctla4 on the surface of T cells have been linked to a state of T cell exhaustion, which contributes to immunosuppression in individuals with acute sepsis.[32] This suggests that Ctla4 may be a pivotal factor in the immunosuppressive phase of sepsis, potentially modulating the immune response by influencing T-lymphocyte activity. Studies have

shown that Atp4a is a key gene in gastric acid secretion, which is not directly related to ALI in sepsis; it may indirectly affect the process of inflammation and immune response.[33,34] CXCL10, a chemokine ligand, modulated the inflammatory response by engaging with its receptor CXCR3. This interaction is crucial for recruitment and activation of inflammatory cells. In sepsis-induced ALI, the CXCL10-CXCR3 axis has been implicated in the exacerbation of lung injury through its role in immune cell trafficking and pro-inflammatory signaling.[35,36] It has been proposed that UMI-77 exerts its protective effect against sepsis-induced ALI by targeting pivotal genes, including Atp4a, Ido1, Ctla4, and Cxcl10, which in turn influence pathways such as cytokine-cytokine receptor interactions, which play a crucial role in the pathology of the disease.

## Conclusion

In this study, we performed comprehensive analysis using transcriptomics and metabolomics to elucidate the therapeutic mechanism of UMI-77 in sepsis-induced ALI. Our results showed that UMI-77 plays an important protective role by regulating key genes (Atp4a, Ido1, Ctla4, and Cxcl10), thus affecting key metabolites (IMP, thiamine monophosphate, and dTMP) and their targets (Entpd2, Entpd1, Nt5e, and Hprt) involved in key biological processes such as cytokine-cytokine receptor interaction, gastric acid secretion, pyrimidines, and purine metabolism, which are key to the pathogenesis of sepsis-induced ALI. These findings not only deepen our understanding of the pathophysiological mechanisms underlying sepsis-induced ALI but also provide strong evidence for the role of UMI-77 in sepsis-induced ALI. Future studies should validate the clinical potential of UMI-77 and provide a scientific basis for its clinical application. We highlighted a new perspective of UMI-77 as a potential therapeutic agent in the treatment of sepsis and how UMI-77 can provide more effective treatment options by modulating the inflammatory response and improving acute lung injury.

## Abbreviations

ARDS, acute respiratory distress syndrome; ALI, acute lung injury; SPF, specific pathogen-free; LPS, lipopolysaccharide; IDA, information-dependent acquisition mode; QC, quality control; PCA, principal component analysis; OPLS-DA, orthogonal partial least squares discriminant analysis; GO, Gene Ontology; FDR, false discovery rate; dTMP, thymidine 3',5'-cyclic monophosphate; IMP, inosine 5'-monophosphate.

## Acknowledgments

The authors express their gratitude to Shanghai Biotree Biotech Co., Ltd. for their support in analyzing UPLC-MS data.

## Funding

The Project was supported by "Pioneer" and "Leading Goose" R&D Program of Zhejiang (2023C03083), Zhejiang Provincial Medical and Health Science and Technology Plan Project (2024KY1823), the University established medical special scientific research project (G2023FSXY03) and the Clinical Research Fund project of Clinical Rational Drug Use Committee of Zhejiang Medical Doctor Association (YS2022-2-008).

## Disclosure

The authors report no conflicts of interest in this work.

## References

1. Li ZG, Scott MJ, Brzoska T, et al. Lung epithelial cell-derived IL-25 negatively regulates LPS-induced exosome release from macrophages. *Mil Med Res*. 2018;5(1):24. doi:10.1186/s40779-018-0173-6
2. Akpinar E, Kutlu Z, Kose D, et al. Protective effects of idebenone against sepsis induced acute lung damage. *J Invest Surg*. 2022;35(3):560–568. doi:10.1080/08941939.2021.1898063
3. Salimi U, Dummula K, Tucker MH, Dela Cruz CS, Sampath V. Postnatal sepsis and bronchopulmonary dysplasia in premature infants: mechanistic insights into "new BPD". *Am J Respir Cell Mol Biol*. 2022;66(2):137–145. doi:10.1165/rcmb.2021-0353PS
4. Dos Santos CC, Amatullah H, Vaswani CM, et al. Mesenchymal stromal (stem) cell therapy modulates miR-193b-5p expression to attenuate sepsis-induced acute lung injury. *Eur Respir J*. 2022;59(1). doi:10.1183/13993003.04216-2020
5. Lv X, Zhang XY, Zhang Q, et al. lncRNA NEAT1 aggravates sepsis-induced lung injury by regulating the miR-27a/PTEN axis. *Lab Invest*. 2021;101(10):1371–1381. doi:10.1038/s41374-021-00620-7

6. Chen R, Cao C, Liu H, et al. Macrophage Sprouty4 deficiency diminishes sepsis-induced acute lung injury in mice. *Redox Biol*. 2022;58:102513. doi:10.1016/j.redox.2022.102513
7. Mallick DJ, Soderquist RS, Bates D, Eastman A. Confounding off-target effects of BH3 mimetics at commonly used concentrations: MIM1, UMI-77, and A-1210477. *Cell Death Dis*. 2019;10(3):185. doi:10.1038/s41419-019-1426-3
8. Liu JW, Zhu ZC, Li K, Wang HT, Xiong ZQ, Zheng J. UMI-77 primes glioma cells for TRAIL-induced apoptosis by unsequestering Bim and Bak from Mcl-1. *Mol Cell Biochem*. 2017;432(1–2):55–65. doi:10.1007/s11010-017-2997-x
9. Cen X, Xu X, Xia H. Targeting MCL1 to induce mitophagy is a potential therapeutic strategy for Alzheimer disease. *Autophagy*. 2021;17(3):818–819. doi:10.1080/15548627.2020.1860542
10. Xu Y, Chen Q, Jiang Y, Liang X, Wang T, Xu Y. UMI-77 modulates the complement cascade pathway and inhibits inflammatory factor storm in sepsis based on TMT proteomics and inflammation array glass chip. *J Proteome Res*. 2023;22(11):3464–3474. doi:10.1021/acs.jproteome.3c00317
11. Thompson O, von Meyenn F, Hewitt Z, et al. Low rates of mutation in clinical grade human pluripotent stem cells under different culture conditions. *Nat Commun*. 2020;11(1):1528. doi:10.1038/s41467-020-15271-3
12. Xu J, Chen Y, Zhang R, et al. Global metabolomics reveals potential urinary biomarkers of esophageal squamous cell carcinoma for diagnosis and staging. *Sci Rep*. 2016;6:35010. doi:10.1038/srep35010
13. Xu Y, Shen B, Pan X, et al. Palmatine ameliorated lipopolysaccharide-induced sepsis-associated encephalopathy mice by regulating the microbiota-gut-brain axis. *Phytomedicine*. 2024;124:155307. doi:10.1016/j.phymed.2023.155307
14. Mohammed A, Cui Y, Mas VR, Kamaleswaran R. Differential gene expression analysis reveals novel genes and pathways in pediatric septic shock patients. *Sci Rep*. 2019;9(1):11270. doi:10.1038/s41598-019-47703-6
15. Zhang S, Hwaiz R, Rahman M, Herwald H, Thorlacius H. Ras regulates alveolar macrophage formation of CXC chemokines and neutrophil activation in streptococcal M1 protein-induced lung injury. *Eur J Pharmacol*. 2014;733:45–53. doi:10.1016/j.ejphar.2014.03.029
16. He S, Jiang X, Yang J, et al. Nicotinamide mononucleotide alleviates endotoxin-induced acute lung injury by modulating macrophage polarization via the SIRT1/NF-kappaB pathway. *Pharm Biol*. 2024;62(1):22–32. doi:10.1080/13880209.2023.2292256
17. Xia W, Pan Z, Zhang H, Zhou Q, Liu Y. ERRalpha protects against sepsis-induced acute lung injury in rats. *Mol Med*. 2023;29(1):76. doi:10.1186/s10020-023-00670-1
18. Kitsiouli E, Tenopoulou M, Papadopoulos S, Lekka ME. Phospholipases A2 as biomarkers in acute respiratory distress syndrome. *Biomed J*. 2021;44(6):663–670. doi:10.1016/j.bj.2021.08.005
19. Das UN. Essential fatty acids and their metabolites in the pathobiology of inflammation and its resolution. *Biomolecules*. 2021;11(12). doi:10.3390/biom11121873
20. Li C, Qi X, Xu L, et al. Preventive effect of the total polyphenols from nymphaea candida on sepsis-induced acute lung injury in mice via gut microbiota and NLRP3, TLR-4/NF-kappaB pathway. *Int J Mol Sci*. 2024;25(8). doi:10.3390/ijms25084276
21. Slim MA, Turgman O, van Vught LA, van der Poll T, Wiersinga WJ. Non-conventional immunomodulation in the management of sepsis. *Eur J Intern Med*. 2024;121:9–16. doi:10.1016/j.ejim.2023.10.032
22. Byun S, Park C, Suh JY, Witte CP, Rhee S. Structure, cooperativity and inhibition of the inosine 5'-monophosphate-specific phosphatase from Saccharomyces cerevisiae. *FEBS J*. 2024;291(9):1992–2008. doi:10.1111/febs.17093
23. Wang S, Tan KS, Beng H, et al. Protective effect of isosteviol sodium against LPS-induced multiple organ injury by regulating of glycerophospholipid metabolism and reducing macrophage-driven inflammation. *Pharmacol Res*. 2021;172:105781. doi:10.1016/j.phrs.2021.105781
24. Zahr NM, Mayer D, Vinco S, et al. In vivo evidence for alcohol-induced neurochemical changes in rat brain without protracted withdrawal, pronounced thiamine deficiency, or severe liver damage. *Neuropsychopharmacology*. 2009;34(6):1427–1442. doi:10.1038/npp.2008.119
25. Chon J, Stover PJ, Field MS. Targeting nuclear thymidylate biosynthesis. *Mol Aspects Med*. 2017;53:48–56. doi:10.1016/j.mam.2016.11.005
26. Jin Q, Xie X, Zhai Y, Zhang H. Mechanisms of folate metabolism-related substances affecting Staphylococcus aureus infection. *Int J Med Microbiol*. 2023;313(2):151577. doi:10.1016/j.ijmm.2023.151577
27. Hosoyamada M, Tomioka NH, Ohtsubo T, Ichida K. Xanthine oxidoreductase knockout mice with high HPRT activity were not rescued by NAD(+) replenishment. *Nucleosides Nucleotides Nucleic Acids*. 2020;39(10–12):1465–1473. doi:10.1080/15257770.2020.1725044
28. St Hilaire C, Ziegler SG, Markello TC, et al. NT5E mutations and arterial calcifications. *N Engl J Med*. 2011;364(5):432–442. doi:10.1056/NEJMoa0912923
29. Grubisic V, Perez-Medina AL, Fried DE, et al. NTPDase1 and −2 are expressed by distinct cellular compartments in the mouse colon and differentially impact colonic physiology and function after DSS colitis. *Am J Physiol Gastrointest Liver Physiol*. 2019;317(3):G314–G332. doi:10.1152/ajpgi.00104.2019
30. Leite RO, Albertino LG, Sperandio LMS, et al. Evaluation of variants in the ENTPD1 and ENTPD2 genes in athletic horses with exercise-induced pulmonary haemorrhage. *BMC Vet Res*. 2024;20(1):346. doi:10.1186/s12917-024-04192-8
31. Lerch S, Schefold JC, Spinetti T. The role of kynurenines produced by indolamine-2,3-dioxygenase 1 in sepsis. *Pharmacology*. 2022;107(7–8):359–367. doi:10.1159/000523965
32. Patil NK, Guo Y, Luan L, Sherwood ER. Targeting immune cell checkpoints during sepsis. *Int J Mol Sci*. 2017;18(11). doi:10.3390/ijms18112413
33. Judd LM, Andringa A, Rubio CA, Spicer Z, Shull GE, Miller ML. Gastric achlorhydria in H/K-ATPase-deficient (Atp4a(-/-)) mice causes severe hyperplasia, mucocystic metaplasia and upregulation of growth factors. *J Gastroenterol Hepatol*. 2005;20(8):1266–1278. doi:10.1111/j.1440-1746.2005.03867.x
34. Liu W, Yang LJ, Liu YL, et al. Dynamic characterization of intestinal metaplasia in the gastric corpus mucosa of Atp4a-deficient mice. *Biosci Rep*. 2020;40(2). doi:10.1042/BSR20181881
35. Herzig DS, Driver BR, Fang G, Toliver-Kinsky TE, Shute EN, Sherwood ER. Regulation of lymphocyte trafficking by CXC chemokine receptor 3 during septic shock. *Am J Respir Crit Care Med*. 2012;185(3):291–300. doi:10.1164/rccm.201108-1560OC
36. Huang H, Zhou H, Wang W, et al. Prediction of acute kidney injury, sepsis and mortality in children with urinary CXCL10. *Pediatr Res*. 2022;92(2):541–548. doi:10.1038/s41390-021-01813-y